Soil Dynamics and Earthquake Engineering 75 (2015) 76–86

Contents lists available at ScienceDirect

Soil Dynamics and Earthquake Engineering

journal homepage: www.elsevier.com/locate/soildyn

Applicability of existing empirical shear wave velocity correlations to seismic cone penetration test data in Christchurch New Zealand

Christopher R. McGann [a,*], Brendon A. Bradley [b], Merrick L. Taylor [b], Liam M. Wotherspoon [c], Misko Cubrinovski [b]

[a] Department of Civil and Environmental Engineering, Washington State University, PO Box 642910, Pullman, WA 99194, USA
[b] Department of Civil and Natural Resources Engineering, University of Canterbury, Private Bag 4800, Christchurch, New Zealand
[c] Department of Civil and Environmental Engineering, The University of Auckland, Private Bag 92019, Auckland, New Zealand

ARTICLE INFO

Article history:
Received 15 April 2014
Received in revised form
10 February 2015
Accepted 27 March 2015

Keywords:
Cone penetration test (CPT)
Seismic piezocone (SCPTu)
Shear wave velocity
Soil age effects

ABSTRACT

Seismic piezocone (SCPTu) data compiled from 86 sites in the greater Christchurch, New Zealand area are used to evaluate several existing empirical correlations for predicting shear wave velocity from cone penetration test (CPT) data. It is shown that all the considered prediction models are biased towards overestimation of the shear wave velocity of the Christchurch soil deposits, demonstrating the need for a Christchurch-specific shear wave velocity prediction model (McGann et al., 2014) [1]. It is hypothesized that the unique depositional environment of the considered soils and the potential loss of soil ageing effects brought about by the 2010–2011 Canterbury earthquake sequence are the primary source of the observed prediction bias.

1. Introduction

The small strain shear modulus is a fundamental soil property required for characterizing the seismic response of surficial soils as it defines the shear stress–strain response at low strain levels and is often used to define normalized models to describe the reduction of the soil shear modulus with increasing levels of strain. Due to this association with low strain levels, the small strain shear modulus is highly susceptible to disturbances caused by sampling and laboratory reconsolidation, therefore, it is difficult to directly measure and values of the small strain shear modulus are often obtained via measurements of the in situ shear wave velocity, V_s, which is fundamentally related to the small strain shear modulus through the elastic wave propagation equation [2].

There are numerous techniques available for obtaining in situ measurements of V_s, including crosshole, downhole, and uphole techniques [3,4]; active-source surface wave techniques such as spectral analysis of surface waves [5] and multichannel analysis of surface waves [6]; passive-source surface wave techniques such as linear [7,8] and microtremor array methods [9,10]; the seismic cone penetration test (SCPT) [11]; and suspension logging [12]. These direct measurement approaches all have specific advantages and disadvantages relative to each other, however, one drawback that is common to these methods in general is the need for specialized equipment and training. Due to these requirements, such measurements are not commonly made during site characterization efforts for projects of lower relative importance. As a result, there is often a lack of site-specific V_s data for such sites and a general scarcity of data for use in region-wide characterization efforts such as the development of regional ground shaking hazard maps.

Direct measurement of V_s is always preferable to indirect estimation, however, due to the noted difficulties with obtaining direct measurements for a particular site, or on the scale necessary for a region-wide characterization, correlations of V_s with soil data obtained from common site investigation techniques such as the standard penetration test (SPT) or cone penetration test (CPT) are useful. Many such correlations have been developed in the past based on various CPT-based predictor variables for various soil types from locations around the world [13–19]. Wair et al. [20] provide a good general overview of these previous CPT-based efforts as well as similar correlations developed using SPT resistance data as predictor variables.

A detailed characterization of the subsurface V_s profile for the greater Christchurch, New Zealand area, is an essential tool to aid in identifying and understanding the physical processes resulting in the strong ground motions observed in the 2010–2011 Canterbury earthquake sequence [21–26]. While in situ measurement of V_s is impractical on the scale necessary for a full characterization of the region, measurements made at selected sites can be used to

* Corresponding author. Tel. +1 509 335 7320.
E-mail addresses: christopher.mcgann@wsu.edu (C.R. McGann), brendon.bradley@canterbury.ac.nz (B.A. Bradley), merrick.taylor@pg.canterbury.ac.nz (M.L. Taylor), l.wotherspoon@auckland.ac.nz (L.M. Wotherspoon), misko.cubrinovski@canterbury.ac.nz (M. Cubrinovski).

http://dx.doi.org/10.1016/j.soildyn.2015.03.021
0267-7261/

establish a region-specific relationship between measured V_s and CPT data. When combined with the large existing local CPT data set [27], such a correlation can be used to produce the desired description of the near surface V_s profile of the Christchurch region [28]. In this paper, data obtained using SCPTu devices [11] at 86 sites located throughout the greater Christchurch area are used to establish the need for a Christchurch-specific CPT–V_s correlation through an assessment of the applicability of existing CPT–V_s models developed elsewhere to describing the strength-to-stiffness relationship for the soils and site conditions found in the Christchurch region. The compiled SCPTu database is first presented, including the spatial distribution of sites, data processing, and overall database statistics. Existing CPT–V_s correlations are then described and the prediction bias when applied to the SCPTu database is examined with respect to various predictor variables. Finally, the specific nature of the soils encountered and the recent Canterbury earthquakes are considered as possibilities for the observed bias in the considered prediction models.

2. Christchurch SCPTu database

Seismic piezocone (SCPTu) data were obtained at 86 sites in the greater Christchurch area and made available through the Canterbury Geotechnical Database [27]. Fig. 1 shows the locations of the SCPTu sites. Those sites closest to central Christchurch are in the main portion of Fig. 1; two sites located beyond the southern boundary of this main portion (in Tai Tapu), and 14 sites located beyond the northern boundary (five in Spencerville and nine in Kaiapoi) are shown in the insets on the right-hand side. As shown in Fig. 1, the majority of the Christchurch sites are located near the Avon River, though there are a number of sites near the Heathcote River or located away from either river system. The Spencerville sites are located along the Styx River and the Kaiapoi sites are near the banks of the Kaiapoi River and Courtenay Stream.

2.1. Geological setting of SCPTu sites

The inset at the left of Fig. 1 shows the centrally located SCPTu sites with respect to the surficial geologic units of the Christchurch urban area [29]. As shown, the surficial soils at these sites are split between the beach, estuarine, lagoonal, dune, and coastal swamp deposits of the Christchurch Formation (blue and grey-blue in Fig. 1 inset) and the fluvial channel and overbank sediment deposits of the Springston Formation (yellow and yellow-grey in Fig. 1 inset). The sites located in Tai Tapu, Spencerville, and Kaiapoi (as well as a site in southern Halswell) are located outside of the bounds of the surficial geologic survey map, and are therefore not included in this inset. These sites are however located within the same surficial geologic units. Of the 86 total SCPTu sites, there are 26 Christchurch Formation sites, 56 Springston Formation sites, and 4 sites located on the boundary of the two. The Christchurch and Springston Formations that exist on the surface of the Canterbury plains date to the Holocene period (deposited $\leq$ 10,000 years before present day). The content of the Springston Formation is primarily well-sorted, rounded gravel within a sand matrix with occasional silt and clay lenses. The Christchurch Formation is composed primarily of blue gravel, sand, shells, sandy silt, clay, peat, and wood [30]. The groundwater table ranged between 0.4 and 3.4 m depth at the SCPTu sites.

2.2. Data processing

Pseudo-interval travel time measurements were made by recording seismic signals at 2 m intervals at each SCPTu site. The horizontal distance between the source plank on the ground surface and the SCPTu rod was reported as 3.6 m in all considered cases. The 2 m sampling interval used in these tests is not ideal (an interval $\leq$ 0.5 m would be preferable), however, the SCPTu data were collected prior to this study and the sampling interval could not be controlled. Shear wave velocities were determined from the seismic signals using the cross-over method [11] for sites with only pre-processed wave data available (40 of 86 SCPTu), and the cross-correlation method [31] for sites with digitized data available (46 of 86 SCPTu). Fig. 2 shows an example of the polarized seismic wave traces that were used to determine V_s via the cross-over method, or to check the V_s returned by the cross-correlation method.

The V_s values determined from the available data are assumed to be constant over the full intervals between the measurements, and the midpoint of each interval is assumed to be the depth of the V_s data point. For comparison between the V_s and CPT data, the geometric mean of the CPT data are determined over the V_s measurement intervals (as the subsequently developed correlation is linear in V_s space), yielding 513 coupled pairs of V_s and CPT data. The use of the geometric mean in variable strata leads only to less precision, however, the variance is low for all cases and no data points were omitted due to excessive variability in the CPT data within the intervals. Averaging the CPT data in this manner helps to alleviate issues associated with comparing measured to CPT-correlated V_s values at locations where the smaller measurement intervals of the CPT ($\approx$ 1–2 cm) detect a localized feature that

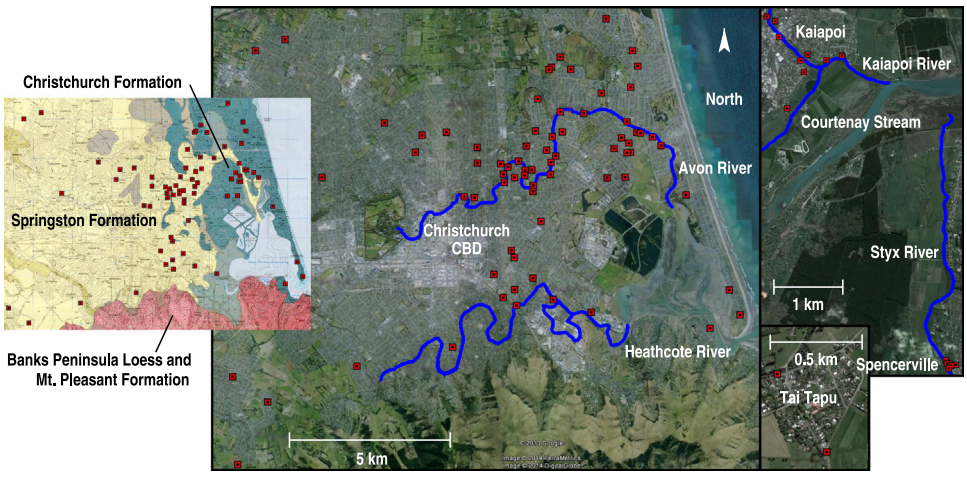

Fig. 1. Map of Christchurch showing the 86 SCPTu site locations (Kaiapoi, Spencerville, and Tai Tapu sites inset at right). The sites are shown in relation to surficial geologic deposits [29] in the inset at left. (For interpretation of the references to color in this figure caption, the reader is referred to the web version of this paper.)

cannot be captured by the much larger V_s measurement intervals, though it should be noted that it may lead to the smearing together of two layers with distinctly different soil types and properties and a corresponding misrepresentation in the liquefaction ageing estimates and I_c values discussed later in this paper. It is also important to note that due to the way that the slanted path traveled by the shear waves emanating from the source changes with depth (e.g., $\approx 45^\circ$ for 2–4 m depths and nearly vertical for $z \geq 10$ m), near-surface measurements may not be consistent with deeper measurements due to material differences on the travel paths and soil anisotropy. Assessments made with the exclusion of measurements at depths $z < 3$ m showed that these data points were not unduly biasing the results, therefore they were retained.

2.3. Distributions of measured and computed SCPTu data

Fig. 3 shows an example of the information provided by each CPT record in the database. In this work, the primary CPT data quantities considered are the raw cone tip resistance q_c (not corrected for pore pressure effect), the frictional cone resistance f_s, the hydrostatic and penetration pore pressures, u_0 and u_2, respectively, and the I_c soil behaviour type index [32]. The soil profile for this site is typical of the database; per I_c, the profile is primarily composed of soil with the behaviour type of clean to silty sand ($1.31 < I_c \leq 2.05$), with relatively small interbedded layers with the behaviour types of silty sands to sandy silts ($2.05 < I_c \leq 2.60$), clayey silts to silty clays ($2.6 < I_c \leq 2.95$), and clays or organic soils ($I_c > 2.95$). Fig. 4 shows the distributions of interval midpoint depth, z, q_c, measured V_s, f_s, and I_c, for the full SCPTu database. The majority of the data are at depths < 16 m; only a small number of sites had V_s measurements below this depth. The I_c plot of Fig. 4 indicates that, as would be expected for profiles similar to that shown in Fig. 3, the majority of the data points have I_c values in the upper half of the clean to silty sand range. The measured V_s values range from 50 m/s to a little over 300 m/s. Some of the shallowest intervals had measured $V_s < 50$ m/s due to poor quality in the uppermost SCPTu signals (typically at 1–2 m depth). These data points were omitted due to lack of confidence in the accuracy of the upper signals. In these cases, the subsequent data points were retained as the lower signals were generally of higher quality.

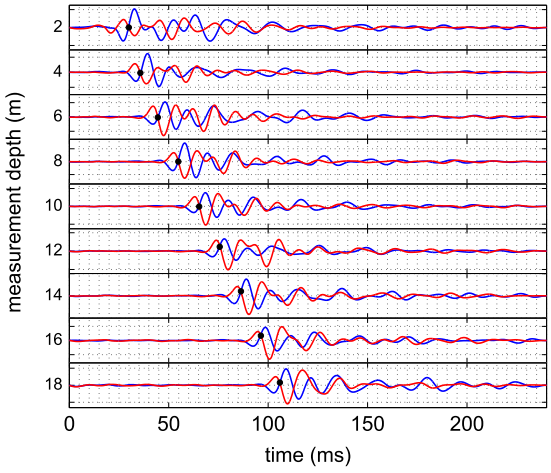

Fig. 2. Example set of seismic wave traces for site in Christchurch SCPTu database. Red and blue lines indicate polarized pairs of waves at each depth. Black markers indicate example cross-over points. (For interpretation of the references to color in this figure caption, the reader is referred to the web version of this paper.)

Fig. 5 shows the distribution of SCPTu test dates over the 15 month period between August 2010 and October 2011. Approximately 60% of the tests in the SCPTu database were performed in the months following the 4 September 2010 M_w7.1 earthquake in areas where liquefaction occurred [26]. These 2010 tests were part of the initial efforts to assess the viability for rebuilding in liquefaction-affected areas following the September earthquake, and are largely located in areas of marginal to severe liquefaction vulnerability for this reason (TC3 and red zone, respectively, according to the residential land zoning categories used by the Christchurch Earthquake Recovery Authority (CERA) [33]). With respect to the maps of Fig. 1, these 2010 tests comprise the sites in Tai Tapu, Spencerville, Kaiapoi and the western suburbs of Christchurch along with a few coastal locations and the majority of the Avon River sites. The SCPTu tests that took place after the 22 February 2011 M_w6.2 earthquake are not as concentrated in the residential red zone areas, as these regions had essentially been defined and designated for abandonment by the time of the second earthquake. The 2011 tests in the SCPTu database are all located within the Christchurch urban area, somewhat evenly divided between the Avon and Heathcote river systems. Overall, approximately 40% of the sites are located within the red zone, 50% of the sites are located in TC3 areas, and the remaining 10% are located in other residential designations (primarily TC2).

3. Review of selected CPT–V_s correlations

Substantial research has been conducted to develop and evaluate correlations between V_s and CPT data. Such efforts can

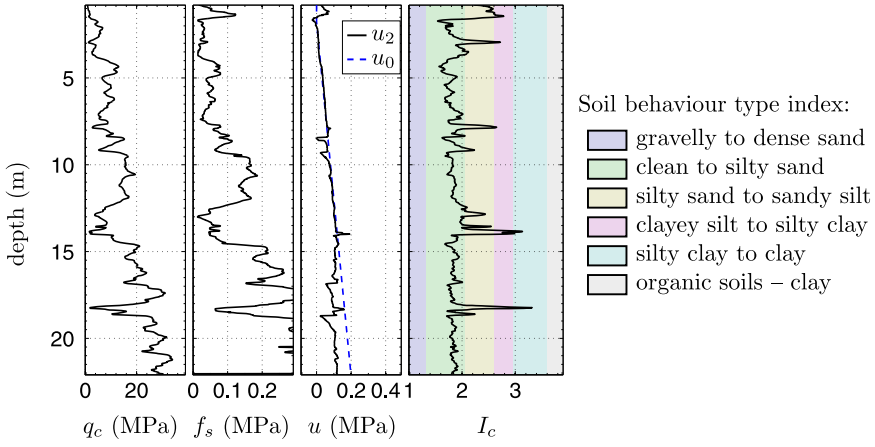

Fig. 3. Example CPT data traces for site in Christchurch SCPTu database. Shaded I_c regions based on soil behaviour type zones of [32]. The groundwater table at this site was reported at 1.8 m depth.

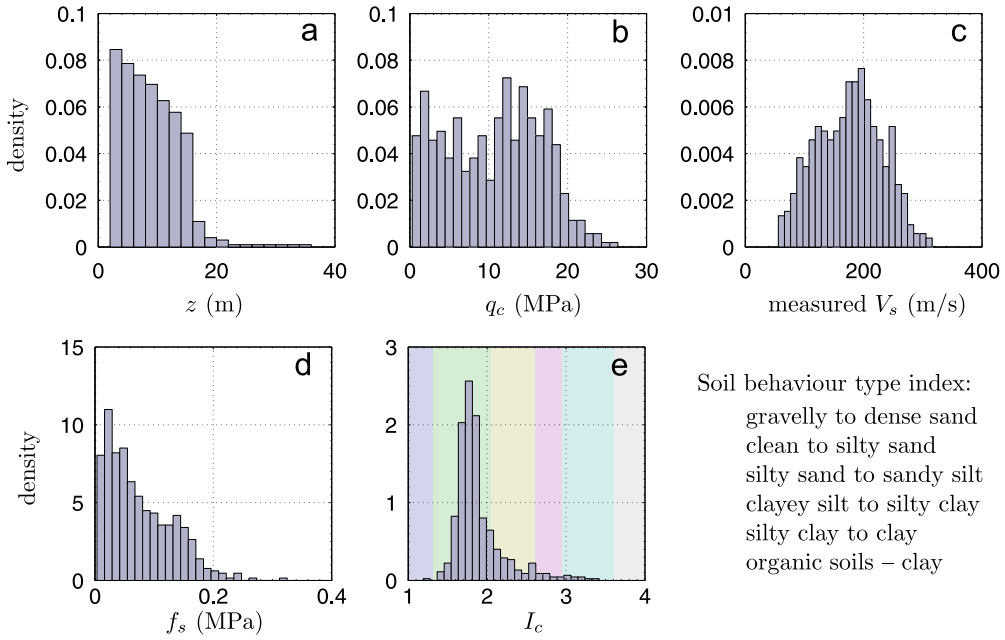

Fig. 4. Density distributions of (a) midpoint depth, z; (b) q_c; (c) measured V_s; (d) f_s; and (e) I_c.

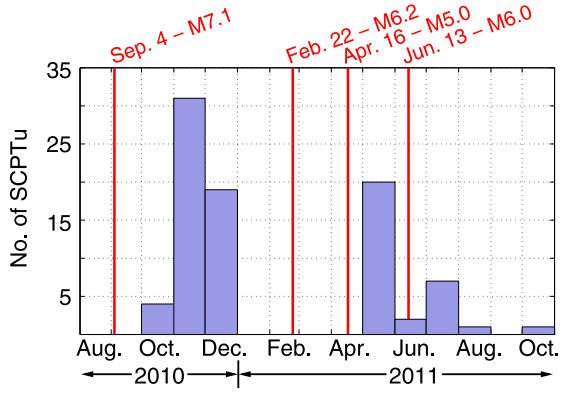

Fig. 5. Distribution of SCPTu test dates (binned by month) with reference to dates of significant Christchurch earthquakes.

be divided into three categories based on the considered soil type: (1) correlations for cohesive soils [e.g., 18]; (2) correlations for cohesionless soils [e.g., 16,17]; and (3) general soil correlations that consider both cohesive and cohesionless soil sites and a predictor variable (e.g., I_c) which can account for differences in soil type [e.g., 19,13–15]. Of these three categories, the general soil correlations are the most appealing as they are simpler to apply and have been shown to perform similar to soil type-specific correlations in predicting V_s for general soil profiles [20]. Four recently developed general soil CPT–V_s correlations derived from relatively independent data sets are considered herein [13–15]. The CPT–V_s correlations from each work are presented in the discussion below with a brief summary of the characteristics of the underlying databases used in their development.

3.1. Andrus et al. (2007) CPT–V_s correlations

Andrus et al. [13] considered V_s and CPT measurements for general soil deposits with various geologic ages as part of a larger study of the effects of deposit age on shear wave velocity. Excluding the Tertiary-age sites that are not applicable to the current study, the considered database included 185 data pairs (72 Holocene, 113 Pleistocene). Two applicable CPT–V_s correlations are presented here, one based on the Holocene-age data only, and the other based on the combined Holocene–Pleistocene database that includes a scaling factor based on the age of the particular soil deposit to which the correlation is applied. The Holocene-only correlation has the following form:

$$V_s = 2.27 q_t^{0.412} I_c^{0.989} z^{0.033} \quad (1)$$

where z is the depth below the ground surface in metres and q_t is the cone tip resistance corrected for pore pressures acting behind the cone tip [34] expressed in units of kPa.

The combined Holocene–Pleistocene correlation has the following form:

$$V_s = 2.62 A q_t^{0.395} I_c^{0.912} z^{0.124} \quad (2)$$

where A is a scaling factor that depends on soil deposit age ($A=0.92$ for Holocene-age sites, $A=1.12$ for Pleistocene sites) and the unit restrictions of Eq. (1) apply. The majority of shear wave velocity measurements were obtained using SCPT (apart from 14 crosshole tests and 6 suspension logger measurements). The CPT soundings for the Holocene sites had a range of soil behaviour type index of $1.19 \le I_c \le 4.0$, with all data pairs at depths $z \le 10$ m. The Pleistocene CPT soundings had a range of soil behaviour type index of $1.16 \le I_c \le 3.25$, with 58 data pairs at depths $z \le 10$ m, 52 pairs at depths $10 < z < 20$ m, and 3 pairs at depths $z \ge 20$ m. Data pairs at depths $z < 3$ m were omitted from both data sets.

3.2. Hegazy and Mayne (2006) CPT–V_s correlation

Hegazy and Mayne [14] developed a CPT–V_{s1} correlation based on 558 data pairs taken from a combined database composed of 31 clay soil sites [18], 30 general soil sites [19], and 12 additional general soil sites. The presented correlation was developed in terms of V_{s1}, the normalized shear wave velocity [35]. When rearranged to solve for V_s the correlation has the following form:

$$V_s = 0.0831 Q_{tn} e^{1.786 I_c} \left(\frac{\sigma'_{v0}}{p_a}\right)^{0.25} \quad (3)$$

where Q_{tn} is the normalized cone tip resistance [32,36], σ'_{v0} is the initial vertical effective stress, e is the natural exponent, and other

terms are as previously defined. The database used to develop this correlation had a range of soil behaviour type index of $1.0 \le I_c \le 4.8$. The in situ V_s measurements were made using a variety of techniques, including SCPT, downhole tests, crosshole tests, and spectral analysis of surface waves (SASW). No trends in the relationship between estimated V_s values and the various measurement methods were reported.

3.3. Robertson (2009) CPT–V_s correlation

Robertson [15] developed a CPT–V_s correlation based on a global set of 1035 pairs of V_s and CPT measurement data from predominantly Holocene and Pleistocene-age general soil sites of the following form:

$$V_s = \left[10^{0.55I_c + 1.68}\left(\frac{q_t - \sigma_{v0}}{p_a}\right)\right]^{0.5} \tag{4}$$

where σ_{v0} is the initial vertical total stress, p_a is the atmospheric pressure, and the other terms are as previously defined. This correlation was obtained from a database of CPT soundings with a mean $Q_{tn} = 57$, and a range of $0.67 \le Q_{tn} \le 577$; a mean friction ratio [37], $F_r = 3.13\%$, with a range of $0.15 \le F_r \le 13.13\%$; and a mean $\sigma'_{v0} = 190$ kPa, with a range of $19 \le \sigma'_{vo} \le 580$ kPa. The techniques used to measure the in situ V_s at these sites are not detailed.

4. Evaluation of selected CPT–V_s correlations

The general soil CPT–V_s correlations discussed in the previous section were applied to the 86 CPT soundings in the SCPTu database for the greater Christchurch area, and the predicted V_s profiles for each correlation compared to the measured V_s values at each site. Fig. 6 shows a comparison between the estimated and measured V_s profiles for a typical site from the SCPTu database. As shown, the existing correlations tend to overestimate the measured V_s values to varying degrees, though the essential form of the V_s profile suggested by the measured values (an increase of V_s with depth) is captured reasonably well by all three correlations. The trend between the measured and estimated V_s values in Fig. 6 is representative of the full database. Similar plots are available for the full set of 86 SCPTu sites in [38].

To quantify the applicability of each existing correlation to Christchurch soil deposits, the V_s prediction bias is defined in terms of the ratio of the estimated to the measured V_s value at each data point, i.e.,

$$V_s \text{ bias} = \frac{\text{estimated } V_s}{\text{measured } V_s} \tag{5}$$

When defined in this manner, a V_s bias > 1.0 represents an overestimation of the measured V_s and a V_s bias < 1.0 represents an underestimation. Fig. 7 summarizes the general performance of the considered shear wave velocity correlations for the Christchurch SCPTu data set. The histogram plots in Fig. 7 show the distribution of the bias for each correlation and provide the mean, μ, and coefficient of variation, COV, of a normal distribution fit to the residual data. The scatter plots compare the measured and estimated V_s and provide the coefficient of determination, r^2, values. The marker colour in these plots corresponds to the I_c of each data pair as indicated.

Fig. 7(a) and (b) compares the performance of the two considered CPT–V_s correlations of Andrus et al. [13]. Of the two, the Holocene-soils correlation appears to be most applicable to the current data set. The mean bias for the Holocene-only correlation is closer to 1.0, and though the 16.8% COV for this case is larger, the Holocene-only correlation provides the more balanced overall bias, tending to overestimate the lower measured V_s values and underestimate the higher V_s values, whereas the Holocene–Pleistocene correlation tends to systematically overestimate the measured V_s values. This systematic overestimation for the combined correlation is likely due to the influence of the naturally higher in situ V_s values for the Pleistocene-age data pairs on the regression.

The Hegazy and Mayne [14] correlation of Fig. 7(d) appears to be the least applicable to the Christchurch soils; with a mean bias $\mu = 1.22$, bias COV = 21.1%, and $r^2 = 0.70$, this correlation displays the most spread of the four estimation methods and most poorly represents the measured data. The Robertson [15] correlation shown in Fig. 7(c) returns a narrower range of estimated V_s and a better representation of the measured V_s data, but systematically overestimates the measured values, leading to the largest mean bias of $\mu = 1.26$. The Holocene-only correlation of [13] appears to be more applicable to the current data set than either of the correlations shown in Fig. 7(c) and (d), with the lowest mean bias, $\mu = 1.12$, a lower COV, and the highest coefficient of determination at $r^2 = 0.82$.

Fig. 8 shows how the V_s prediction bias varies with q_c, f_s, and interval midpoint depth, z, for the three indicated existing correlations (the Holocene-only correlation of [13] is used hereafter unless otherwise noted). The black lines in these plots represent the moving averages (solid line), with 95% confidence intervals (dashed lines), providing a depiction of the trend suggested in these plots. Determining the ranges of these CPT-based variables that display concentrations of high and low bias can aid in understanding why the correlations may or may not be applicable to the current soil deposits, and can help determine which of these terms are important to consider in a Christchurch-specific CPT–V_s correlation.

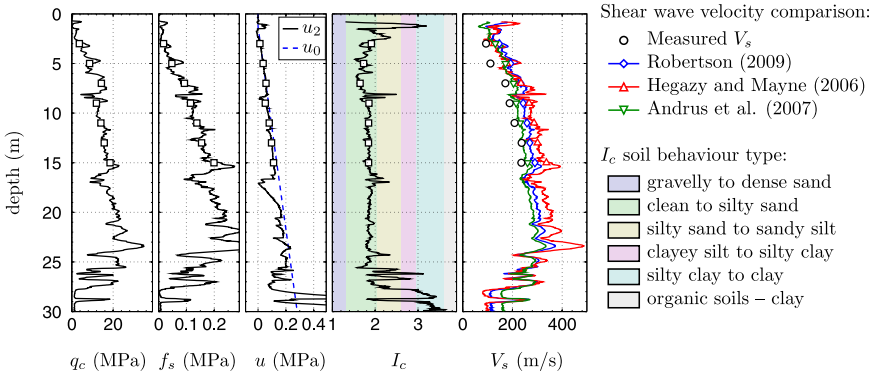

Fig. 6. Example CPT record from SCPTu database with comparison of measured and estimated V_s profiles. Markers for CPT and estimated V_s plots represent geometric mean over V_s measurement intervals.

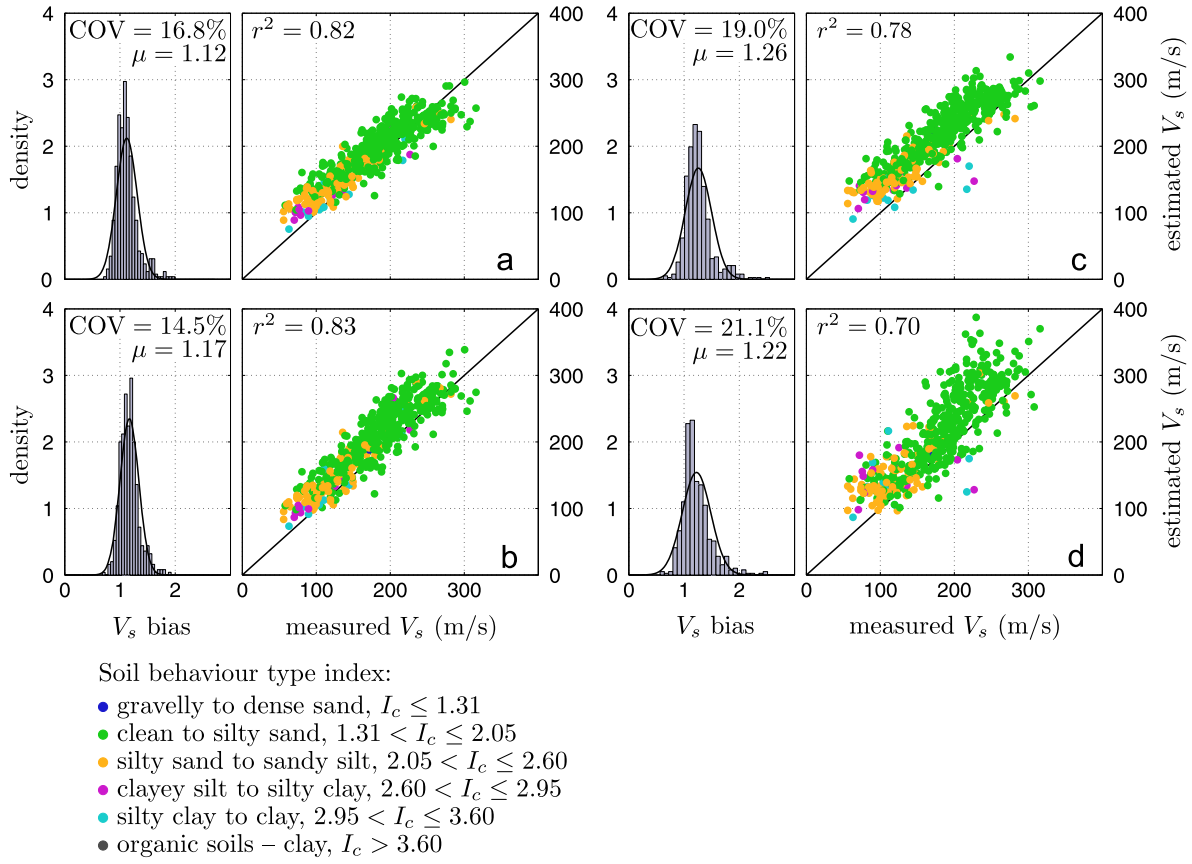

Fig. 7. Performance of existing CPT–V_s correlations in current soils. (a) Andrus et al. [13] Holocene; (b) Andrus et al. [13] Holocene–Pleistocene; (c) Robertson [15]; (d) Hegazy and Mayne [14].

The depth variation plots of Fig. 8 show the most dramatic variations of the three variables considered. As indicated, the overestimation apparent in all three correlations is most prevalent at relatively shallow depths (approximately $z < 4$ m). In contrast, the intermediate range of depths ($4 \le z \le 20$ m) shows a fairly constant average bias. There is a significant decrease in the number of measured V_s data points beyond $z \approx 20$ m; trends in the average bias for these deeper locations may be influenced by this relative lack of data. All three empirical predictions show similar concentrations of bias at the lower end of the cone resistance ranges (approximately $q_c \le 3$ MPa and $f_s \le 0.05$ MPa). Beyond these ranges, the average bias for both the Andrus et al. and Robertson correlations tends to decrease with increasing q_c while remaining relatively constant with increasing f_s. The average correlation bias for the Hegazy and Mayne model tends to increase slightly as q_c increases beyond about 10 MPa, and more significantly as f_s increases beyond about 0.05 MPa. It appears from the plots of Fig. 8 that the zones of larger bias at lower values of q_c and f_s coincide with values of $I_c > 2.0$, indicating that soils with silt or clay behaviour types may be poorly predicted.

The inability of the three correlations to represent the shallow V_s values, and the apparent concentrations of larger bias at low q_c and f_s values, may be due, in part, to extrapolation beyond the original considered data sets. For example, the Andrus et al. [13] study explicitly omitted data with depths $z < 3$ m from the correlation database, thus, this relationship is not applicable to the full range of depths considered in the current study. Extrapolation error however does not appear to account for all of the bias apparent in the existing V_s correlations, as the ranges of CPT measurements and implied soil behaviour types indicated in each work coincide reasonably well with the current data set. Errors associated with the averaging of the CPT data over the 2 m SCPTu measurement intervals may also contribute to the bias, along with the previously mentioned issues arising from changes in the shear wave travel path with depth (especially for shallow depths). Another potential source of bias at shallow depths is the uncertainty associated with CPT resistance data for low confining pressures. The observed bias could also be due to differences between in situ V_s measurement techniques (SCPTu in current study, various in existing correlations), or more likely, due to the region-specific geological history of the soils involved.

Fig. 9 shows how the bias for each correlation varies with the I_c values of the data set. The marker colours in these plots represent the magnitudes of q_c and f_s as indicated. As shown in Fig. 9, the average bias for all three cases increases with increasing I_c for values of $I_c < 2.5$. Beyond this point the bias for the Andrus et al. and Robertson correlations tends to decrease with increasing I_c, while the bias for the Hegazy and Mayne correlation remains relatively constant with increasing I_c. The confidence interval for the Andrus et al. correlation is essentially constant for the considered I_c range, while the results for the other correlations display a clear reduction in confidence for the mean bias as I_c increases and the data points spread apart and become less frequent. As expected, the larger q_c and f_s values are concentrated in the clean-to-silty sand range of the chart, though the inclusion of these magnitudes does not reveal any significant trend in the relationship between I_c and the prediction bias not already noted from the results of Fig. 8.

5. Consideration for age effects

Another source of the bias present in the results of Figs. 8 and 9 could be related to a loss or reduction of age effects (e.g., time

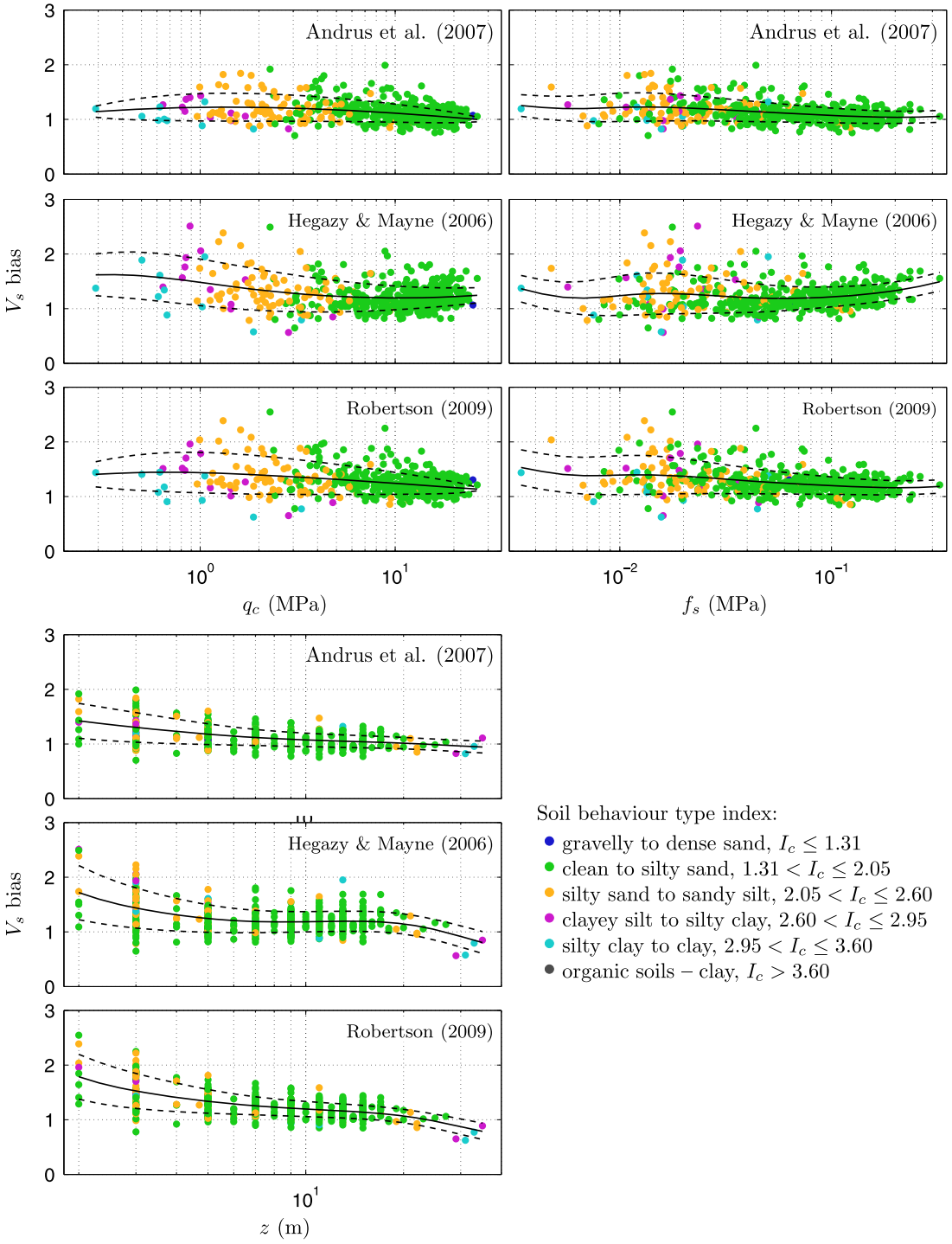

Fig. 8. Variation of V_s bias with raw cone tip resistance, frictional resistance, and depth. Marker colour indicates soil behaviour type index [32] as noted. (For interpretation of the references to color in this figure caption, the reader is referred to the web version of this paper.)

effects on soil micro-structure, reorientation of grains due to load, creep, cementation at grain contact points) in the Christchurch soils brought about by large strains and induced pore pressures associated with the events of the 2010–2011 Canterbury earthquake sequence. Age effects generally lead to an increase in V_s over time, and it is likely that such effects were destroyed or significantly reduced at most of the sites in the SCPTu database from either the Canterbury earthquake sequence or potentially prior significant seismic events. As discussed previously, the SCPTu records that comprise the current database were obtained during various post-earthquake site evaluation efforts used to assess the viability of rebuilding in liquefaction-affected areas, therefore many of the SCPTu sites were located in areas of moderate to severe liquefaction. A complete loss of age effects is expected for soils that liquefied and resedimented, and the concentrated bias in the examined relationships at shallow depths coincides with the soils most susceptible to these phenomena, indicating that the liquefaction associated with the earthquakes may have played a significant role in eliminating age effects in, and reducing the applicability of the existing correlations to, the Christchurch soils.

A previous study on liquefaction resistance corrections for aged sands [39], showed how the ratio of measured to estimated V_s

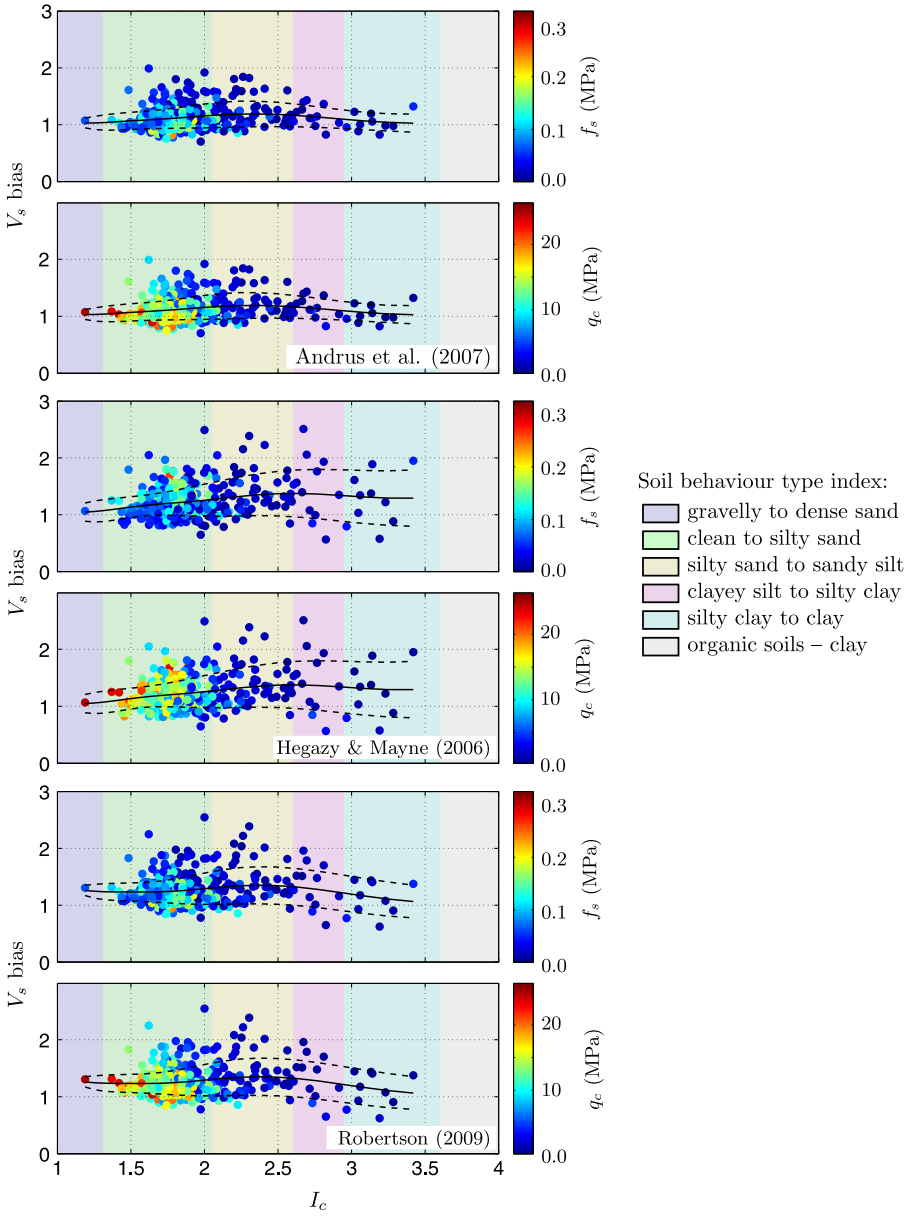

Fig. 9. Variation of V_s bias with I_c soil behaviour type index. Marker colour indicates magnitude of q_c and f_s, and background colour indicates soil behaviour type index zones [32] as noted. (For interpretation of the references to color in this figure caption, the reader is referred to the web version of this paper.)

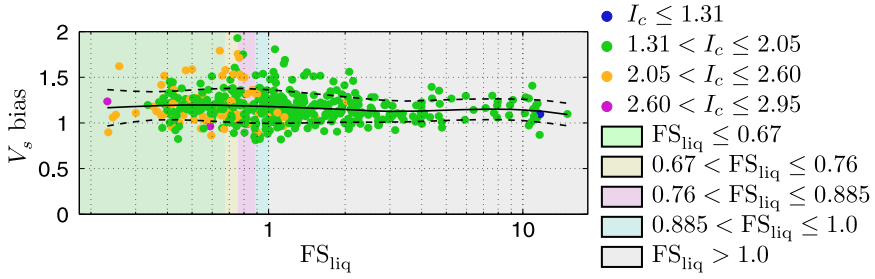

Fig. 10. Variation of V_s bias with estimated factor of safety against liquefaction, $\mathrm{FS_{liq}}$, for Holocene–Pleistocene [13] CPT–V_s correlation.

increases with the apparent age of a soil deposit (time since original deposition or since intervening critical disturbance such as liquefaction) for V_s values estimated using the combined Holocene–Pleistocene CPT–V_s correlation given by Eq. (2). These results indicate that sites with apparent ages beyond the scope considered during the development of the correlation tend to be underestimated (older deposits) or overestimated (younger deposits) on average by the CPT–V_s relationship. To evaluate the current data set in this context, the apparent age of each data pair is defined as the time since initial deposition for locations where

liquefaction did not occur or the time since the most recent occurrence of liquefaction for locations that experienced liquefaction due to the 2010–2011 Canterbury earthquakes.

Original depositional ages are estimated using the minimum age with depth suggested by a chart [40] compiled to describe the age of soils overlying the Riccarton Gravel deposit based on radiocarbon ages of Christchurch soils reported by Brown and Weeber [29]. The time since the most recent occurrence of liquefaction is estimated as the number of days elapsed between the date of the SCPTu test and the most recent earthquake (of the four shown in Fig. 5, 4 September 2010 and 22 February, 16 April, and 13 June 2011) for which the factor of safety against liquefaction, FS_{liq}, as computed using the method of Idriss and Boulanger [41], indicates a high likelihood of liquefaction or significant soil fabric disturbance. To this purpose, fines content, FC, values are estimated from I_c using the Christchurch-specific correlation developed for Avon River soil sites [42]. Data pairs that meet the dual criteria of $I_c > 2.6$ and friction ratio $F_r > 1.0\%$ proposed by Robertson and (Fear) Wride [32] are excluded from this age effect study.

Fig. 10 shows the variation of V_s bias, with FS_{liq} for the Holocene–Pleistocene CPT–V_s correlation of Andrus et al. [13]. As shown, this correlation overpredicts the in situ V_s on average over the full range of FS_{liq} values. The background colours and accompanying FS_{liq} ranges noted in Fig. 10 correspond to the likelihood of liquefaction classes summarized in Table 1. Taylor [43] developed these likelihood classes [44] based on probabilities of liquefaction, P_{liq}, computed for FS_{liq} values returned by the deterministic liquefaction potential evaluation method of Idriss and Boulanger [41] in a manner similar to that done by Ku et al. [45] for the liquefaction potential evaluation method of Robertson and (Fear) Wride [32].

Figs. 11 and 12 show the variation of measured to estimated V_s ratio, MEVR [39], for the Holocene–Pleistocene [13] CPT–V_s correlation applied to the sand data points of Andrus et al. [39] (black markers) and the current Christchurch SCPTu database sites (coloured markers). The MEVR in this context is defined as the reciprocal of the V_s bias given in Eq. (5). The solid black line in each plot represents the mean regression line fit to the existing data, given by Andrus et al. [39] as

$$\text{MEVR} = \frac{\text{measured } V_s}{\text{estimated } V_s} = 0.0820 \log_{10}(t) + 0.935 \tag{6}$$

where t is the time. The dashed black lines show $+/-$ one standard deviation from the mean regression line. The time since critical disturbance for the current data set shown in Fig. 11 is defined as $FS_{liq} \leq 0.885$ based on the liquefaction likelihood classes of Table 1, which indicates that locations with factors of safety > 0.885 are unlikely or almost certain not to liquefy for the given events. With this definition for critical disturbance, the current data set is split fairly evenly into two groupings. One containing the data points where liquefaction was deemed likely to have occurred and the apparent ages are less than one year, and one with the data points deemed undisturbed by the $FS_{liq} \leq 0.885$ criteria where the apparent ages are the original depositional ages ($\approx$ 1000–10,000 years) estimated from the chart of Cubrinovski and McCahon [40], which assumes that there have been no significant seismic events in the immediate vicinity of the region over this time period. This assumption is not ideal, but given the lack of information with which to more accurately determine the apparent ages for these sites, and recent research supporting this assumption [46,47], it is the most reasonable approach at this time. Fig. 12 shows the same information, but for a different definition of the time since critical disturbance for the current data set. In this case, the critical disturbance is defined as $FS_{liq} \leq 2.0$ which, per Ishihara and Yoshimine [48], roughly corresponds with the point at which non-negligible maximum shear strains develop in sands. For this criterion, the majority of the current data set is considered to have been critically disturbed by one of the events of the Canterbury earthquake sequence, though as shown in Fig. 12 a grouping of undisturbed data points remains. Of the 86 SCPTu locations, 71 sites had at least one data point considered disturbed by the $FS_{liq} \leq 0.885$ criteria, with 63 of these sites coinciding with areas where van Ballegooy et al. [49] reported observations of minor to severe surface manifestations of liquefaction. For the $FS_{liq} \leq 2.0$ criteria, 84 sites had at least one disturbed data point and 72 of these sites coincided with surficial liquefaction observations.

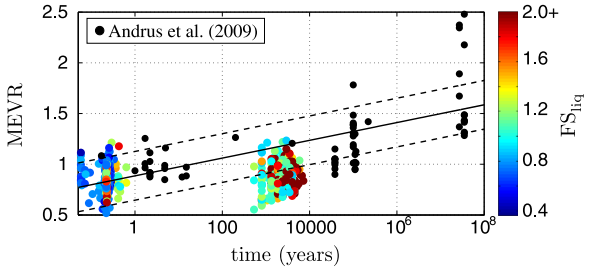

Fig. 11. Variation of MEVR with time since critical disturbance or initial deposition, with critical disturbance defined as $FS_{liq} \leq 0.885$. Marker colour for current data set corresponds to FS_{liq} as indicated. (For interpretation of the references to color in this figure caption, the reader is referred to the web version of this paper.)

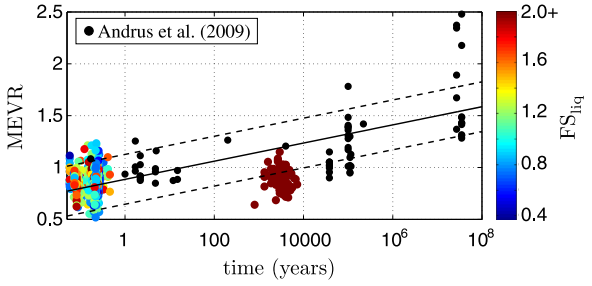

Fig. 12. Variation of MEVR with time since critical disturbance or initial deposition, with critical disturbance defined as $FS_{liq} \leq 2.0$. Marker colour for current data set corresponds to FS_{liq} as indicated. (For interpretation of the references to color in this figure caption, the reader is referred to the web version of this paper.)

Table 1
Liquefaction likelihood classes based on probabilities of liquefaction for FS_{liq} values after [43,44].

Class	Probability	Factor of safety	Likelihood description
5	$0.85 \leq P_{liq}$	$FS_{liq} \leq 0.67$	Almost certain to liquefy
4	$0.65 \leq P_{liq} \leq 0.85$	$0.67 \leq FS_{liq} \leq 0.76$	Very likely to liquefy
3	$0.35 \leq P_{liq} \leq 0.65$	$0.76 \leq FS_{liq} \leq 0.885$	Liquefaction and no liquefaction equally likely
2	$0.15 \leq P_{liq} \leq 0.35$	$0.885 \leq FS_{liq} \leq 1.0$	Unlikely to liquefy
1	$P_{liq} < 0.15$	$1.0 < FS_{liq}$	Almost certain not to liquefy

The results of Figs. 11 and 12 show that the V_s values of the current data set, even the undisturbed locations with apparent ages similar to those used to develop the correlation, are overestimated by the Holocene–Pleistocene [13] correlation. The data points with apparent ages < 1 year appear to follow the trend suggested by the Andrus et al. [39] data set for both considered definitions of critical disturbance, while the data points considered to be undisturbed by both the $FS_{liq} \leq 0.885$ and $FS_{liq} \leq 2.0$ criteria do not follow this trend. This marked difference between the increase in V_s with age displayed by the existing data and the lack of increase displayed by the current data suggests at least two possibilities:

1. All the soils comprising the sites in Christchurch SCPTu database experienced a complete loss or significant reduction in age effects from shear strains and induced pore pressures due to the 2010–2011 earthquakes, regardless of whether liquefaction did or did not occur.
2. The depositional environment or the effect of deposit age on the strength and stiffness of these Christchurch soil sites is unique in some fundamental way. The changes in river paths and groundwater conditions that have taken place during the recent geological history of this region could possibly have contributed to disturbances in the accumulation of age effects. Additionally, estimation of the undisturbed ages from the Cubrinovski and McCahon [40] chart ignores any reduction or loss in age effects brought about by significant seismic events that took place in the region after original deposition but prior to the start of the historical record (about 150 years ago for New Zealand), or known historical events such as the approximately M_w5 earthquake that took place in 1870 [50]. This uncertain effect of past seismic activity on the apparent age of soil deposits is inherent in the Andrus et al. [39] results as well, and the assumption of equality between the apparent and estimated depositional ages for soils undisturbed by known seismic events may hold true in regions of low seismicity or with a long historical record of earthquakes.

In either case, it is clear that the soils in the greater Christchurch area are poorly represented on average by the considered CPT–V_s correlations. It appears that the unique depositional and post-earthquake conditions of these soils contribute significantly to this difference, and as a result, there is a clear need for a region-specific CPT–V_s correlation [1].

6. Conclusions

A database of 86 SCPTu sites was compiled from subsurface explorations performed in the greater Christchurch, New Zealand area following the 2010–2011 Canterbury earthquake sequence. All the considered sites were obtained from CPT soundings made available in the Canterbury Geotechnical Database [27]. These sites are located in areas in which the surficial geologic deposits are from the Christchurch and Springston Formations [29]. In situ shear wave velocities were determined from pseudo-interval travel time data (spaced at 2 m intervals) using the cross-over and cross-correlation approaches. The CPT data were averaged over the V_s measurement intervals using the geometric mean to yield 513 unique pairs of CPT and V_s data for the soils of the Christchurch region.

The Christchurch SCPTu data set was utilized to assess the suitability of four existing CPT–V_s correlations for describing the relationship between CPT data and in situ shear wave velocity for soil deposits in the greater Christchurch area. It was determined that all four correlations produce biased V_s estimates when applied to the CPT soundings of the database, with each existing correlation tending to overestimate the in situ V_s to varying degrees. The Holocene-age correlation of Andrus et al. [13] was found to be the most applicable to the soils of the Christchurch region, displaying the smallest degree of overestimation (12% on average) and the best representation of the current data. Adjustments to account for disturbances to soil ageing effects at the considered soil sites due to the events of the 2010–2011 Canterbury earthquake sequence showed that the observed bias persisted irrespective of the apparent soil age, suggesting that the considered Christchurch soils possess a unique region-specific geologic history that leads to the biased estimates returned by the existing CPT–V_s correlations. These findings suggest that the development of a Christchurch-specific correlation, presented in the companion paper [1], that captures the unique nature of the regional soils will be beneficial to future research efforts.

Acknowledgments

Funding for this work was provided by the New Zealand Earthquake Commission (EQC) and the Natural Hazards Research Platform (NHRP). The authors would also like to thank the Canterbury Geotechnical Database and Perry Drilling Ltd. for providing access to the data used in this study.

References

[1] McGann C, Bradley B, Taylor M, Wotherspoon L, Cubrinovski M. Development of an empirical correlation for predicting shear wave velocity of Christchurch soils from cone penetration test data. Soil Dyn Earthq Eng 2014;00(0):15–27.
[2] Stokoe II K, Santamarina J. Seismic-wave-based testing in geotechnical engineering. In: Proceedings of the international conference on geotechnical and geological engineering, GeoEng 2000. Melbourne, Australia; 2000. p. 1490–1536.
[3] Woods R. Measurement of dynamic soil properties, state of the art report. In: Proceedings of the ASCE specialty conference on earthquake engineering & soil dynamics, vol. 1. Pasadena, USA: California Institute of Technology; 1978. p. 91–178.
[4] Woods R. Borehole methods in shallow seismic exploration. In: Woods R, editors. Geophysical characterization of sites. New Delhi, India: ISSMFE Technical Committee #10; 1994. p. 91–100.
[5] Nazarian S, Stokoe II K. In-situ shear wave velocities from spectral analysis of surface wave tests. In: Proceedings of the eighth world conference on earthquake engineering. San Francisco, CA; 1984. p. 31–8.
[6] Park C, Miller R, Xia J. Multichannel analysis of surface waves. Geophysics 1999;64(3):800–80.
[7] Louie J. Faster, better shear wave velocity to 100 meters depth from refraction microtremor arrays. Bull Seismol Soc Am 2001;91(2):347–64.
[8] Park C, Miller R. Roadside passive multichannel analysis of surface waves (MASW). J Environ Eng Geophys 2008;13(1):1–13.
[9] Tokimatsu K, Shinzawa K, Kuwayama S. Use of short-period microtremors for V_s profiling. J Geotech Eng 1992;118(10):1544–58.
[10] Okada H. The microtremor survey method. Society of Exploration Geophysicists [Suto K, translator]. SEG geophysical monograph series no. 12; 2003.
[11] Robertson P, Campenella R, Gillespie D, Rice A. Seismic CPT to measure in-situ shear wave velocity. J Geotech Eng 1986;112(8):791–804.
[12] Kaneko F, Kanemori T, Tonouchi K. Low-frequency shear wave logging in unconsolidated formations for geotechnical applications. In: Paillet F, Saunders W, editors. Geophysical applications for geotechnical investigations, ASTM STP 1101. Philadelphia, PA, USA: American Society for Testing and Materials; 1990. p. 79–98.
[13] Andrus R, Mohanan N, Piratheepan P, Ellis B, Holzer T. Predicting shear-wave velocity from cone penetration resistance. In: Proceedings of the fourth international conference on earthquake geotechnical engineering, Thessaloniki, Greece. Paper no. 1454; June 25–28, 2007.
[14] Hegazy Y, Mayne P. A global statistical correlation between shear wave velocity and cone penetration data. In: Puppala A, Fratta D, Alshibli K, Pamukcu S, editors. Proceedings of the GeoShanghai, site and geomaterial characterization (GSP 149). Reston, VA: ASCE; 2006. p. 243–8.
[15] Robertson P. Interpretation of cone penetration tests—a unified approach. Can Geotech J 2009;46(11):1337–55.
[16] Sykora D, Stokoe II K. Correlations of in-situ measurements in sands and shear wave velocity. The University of Texas at Austin. Geotechnical engineering report GR83-33; 1983.
[17] Baldi G, Belloti R, Ghionna V, Jamiolkowski M, Lo Presti D. Modulus of sands from CPTs and DMTs. In: Proceedings of the 12th international conference on

soil mechanics and foundation engineering, vol. 1. Rio de Janeiro; 1989. p. 165–70.
[18] Mayne P, Rix G. G_{max}–V_s relationships for clays. Geotech Test J 1993;16(1):54–60.
[19] Hegazy Y, Mayne P. Statistical correlations between V_s and cone penetration data for different soil types. In: Proceedings of the CPT '95, vol. 2. Linköping, Sweden: Swedish Geotechnical Society; 1995. p. 173–8.
[20] Wair B, DeJong J, Shantz T. Guidelines for estimation of shear wave velocity profiles. Berkeley: Pacific Earthquake Engineering Research Center, University of California. PEER report no. 2012/08; 2012.
[21] Bradley B, Cubrinovski M. Near-source strong ground motions observed in the 22 February 2011 Christchurch earthquake. Seismol Res Lett 2011;82(6):853–65.
[22] Bradley B. Strong ground motion characteristics observed in the 4 September 2010 Darfield, New Zealand earthquake. Soil Dyn Earthq Eng 2012;42:32–46.
[23] Bradley B. Ground motions observed in the Darfield and Christchurch earthquakes and the importance of local site response effects. NZ J Geol Geophys 2012;55(3):279–86.
[24] Cubrinovski M, Bradley B, Wotherspoon L, Green R, Bray J, Wood C, et al. Geotechnical aspects of the 22 February 2011 Christchurch earthquake. Bull NZ Soc Earthq Eng 2011;44(4):205–26.
[25] Cubrinovski M, Bray J, Taylor M, Giorgini S, Bradley B, Wotherspoon L, et al. Soil liquefaction effects in the central business district during the February 2011 Christchurch earthquake. Seismol Res Lett 2011;82(6):893–904.
[26] Cubrinovski M, Green R, Allen J, Ashford S, Bowman E, Bradley B, et al. Geotechnical reconnaissance of the 2010 Darfield (Canterbury) earthquake. Bull NZ Soc Earthq Eng 2010;43(4):243–320.
[27] Canterbury Geotechnical Database. ⟨http://canterburygeotechnicaldatabase.projectorbit.com⟩; 2012.
[28] Lee R, Bradley B, Pettinga J, Hughes M, Graves R. Ongoing development of a 3D seismic velocity model of Canterbury, New Zealand for broadband ground motion simulation. In: New Zealand Society for earthquake engineering annual conference, Auckland; March 21–23, 2014. Paper no. 8.
[29] Brown L, Weeber J. Geology of the Christchurch urban area. Lower Hutt. New Zealand: Institute of Geological and Nuclear Sciences Ltd; 1992.
[30] Brown L, Beetham R, Paterson B, Weeber J. Geology of Christchurch, New Zealand. Environ Eng Geosci 1995;1(4):427–88.
[31] Campanella R, Stewart W. Seismic cone analysis using digital signal processing for dynamic site characterization. Can Geotech J 1992;29(3):477–86.
[32] Robertson P, (Fear) Wride C. Evaluation cyclic liquefaction potential using the cone penetration test. Can Geotech J 1998;35(3):442–59.
[33] Canterbury Earthquake Recovery Authority (CERA), ⟨http://cera.govt.nz/land-information/land-zones⟩; 2014.
[34] Campanella R, Gillespie D, Robertson P. Pore pressures during cone penetration testing. In: Proceedings of the second European symposium on penetration testing, ESPOT II. Amsterdam; May 24–27, 1982. p. 507–12.
[35] Robertson P, Woeller D, Finn W. Seismic cone penetration test for evaluating liquefaction potential. Can Geotech J 1992;29(4):686–95.
[36] Zhang G, Robertson P, Brachman R. Estimating liquefaction-induced ground settlements from CPT for level ground. Can Geotech J 2002;39(5):1168–80.
[37] Robertson P. Soil classification using the cone penetration test. Can Geotech J 1990;27(1):151–8.
[38] McGann C, Bradley B, Cubrinovski M, Taylor M, Wotherspoon L. Development and evaluation of CPT–V_s correlation for Canterbury New Zealand soils of the shallow Christchurch and Springston formations. University of Canterbury Research report no. 2014-01; 2014.
[39] Andrus R, Hayati H, Mohanan N. Correcting liquefaction resistance for aged sands using measured to estimated velocity ratio. J Geotech Geoenviron Eng 2009;135(6):735–44.
[40] Cubrinovski M, McCahon I. Foundations of deep alluvial soils. Technical report prepared for the Canterbury Earthquakes Royal Commission; 2011.
[41] Idriss I, Boulanger R. Soil liquefaction during earthquakes. Earthquake Engineering Research Institute (EERI), MNO-12; 2008.
[42] Robinson K, Cubrinovski M, Bradley B. Sensitivity of predicted liquefaction-induced lateral displacements from the 2010 Darfield and 2011 Christchurch earthquakes. In: Proceedings of the 19th New Zealand Geotechnical Society (NZGS) symposium. Queenstown, New Zealand; November 20–23, 2013.
[43] Taylor M. The geotechnical characterisation of Christchurch sands for advanced soil modelling [Ph.D. dissertation]. University of Canterbury, Christchurch, New Zealand; 2014.
[44] Chen C, Juang C. Calibration of SPT- and CPT-based liquefaction evaluation methods. In: Mayne P, Hryciw R, editors. Innovations and applications in geotechnical site characterization: proceedings of sessions of Geo-Denver 2000 (GSP 97). Reston, VA: ASCE; 2000. p. 49–64.
[45] Ku CS, Juang C, Chang CW, Ching J. Probabilistic version of the Robertson and Wride method for liquefaction evaluation: development and application. Can Geotech J 2012;49(1):27–44.
[46] Hornblow S, Quigley M, Nicol A, VanDissen R, Wang N. Paleoseismology of the 2010 Mw 7.1 Darfield (Canterbury) earthquake source, Greendale Fault, New Zealand. Tectonophysics 2014;637:178–90. http://dx.doi.org/10.1016/j.tecto.2014.10.004.
[47] Mackey B, Quigley M. Strong proximal earthquakes revealed by cosmogenic 3He dating of prehistoric rockfalls, Christchurch, New Zealand. Geology 2014;42(11):975–8. http://dx.doi.org/10.1130/G36149.1.
[48] Ishihara K, Yoshimine M. Evaluation of settlements in sand deposits following liquefaction during earthquakes. Soils Found 1992;32(1):173–88.
[49] van Ballegooy S, Malan P, Lacrosse V, Jacka M, Cubrinovski M, Bray J, et al. Assessment of liquefaction-induced land damage for residential Christchurch. Earthq Spectra 2014;30(1):31–55.
[50] Gledhill K, Ristau J, Reyners M, Fry B, Holden C. The Darfield (Canterbury, New Zealand) M_w7.1 earthquake of September 2010: a preliminary seismological report. Seimol Res Lett 2011;82(3):378–86.